

Status of the LHCb experiment

On behalf of the LHCb collaboration
T. Nakada

CERN, CH-1211 Geneva 23, Switzerland
and
IPHE, Université de Lausanne, CH-1015 Lausanne, Switzerland
e-mail: tatsuya.nakada@cern.ch

Received:

Abstract. LHCb is a dedicated experiment to study CP violation and other rare processes in the B meson system at LHC. It is designed to exploit the large sample of B_d and B_s mesons available at LHC by having a trigger system efficient for both leptonic and hadronic final states, particle identification capability over large momentum range and excellent decay time resolution. Recently, the detector has been reoptimized in order to reduce the material budget and to improve the trigger performance. Construction of various detector components is well advancing and the experiment is expected to be ready for data taking from the beginning of the LHC operation.

PACS: 25.70.Ef; 21.60.Gx; 27.30.+t

1 Introduction

In 2001, long awaited CP violation outside of the neutral kaon system was observed in the B^0 and \bar{B}^0 decays into various CP eigenstates generated by the $b \rightarrow c + W^-$ and $\bar{b} \rightarrow \bar{c} + W^+$ tree diagrams, such as $J/\psi K_S^0$ and $\eta_c K_S^0$, by the BABAR [1] and BELLE [2] collaborations. Assuming these decays are dominated by the Standard Model processes, CP asymmetries from those final states yield [3]

$$\sin\phi_d = \begin{cases} 0.741 \pm 0.075 & \text{BABAR} \\ 0.719 \pm 0.082 & \text{BELLE} \end{cases} .$$

The phase ϕ_d is identical to the phase of the B^0 – \bar{B}^0 oscillation amplitude with a phase convention adopted by the often used Wolfenstein's parametrization [4] of the Cabibbo-Kobayashi-Maskawa (CKM) mass mixing matrix [5, 6], where those B^0 and \bar{B}^0 weak decay amplitudes are real. If we assume that only the Standard Model box processes contribute to the B^0 – \bar{B}^0 oscillation, ϕ_d is identical to $-2 \arg V_{td} = 2\beta$ where V_{td} is one of the elements of the CKM matrix. Averaging the two results, one obtains

$$\sin 2\beta = 0.731 \pm 0.055 \quad (\text{from CP violation}). \quad (1)$$

With the same assumption, $|V_{td}|$ can be determined from the B^0 – \bar{B}^0 oscillation frequency Δm_d . Together with $|V_{cb}|$ and $|V_{ub}|$ obtained from various B^0

and \bar{B}^0 decays, β can be determined using the unitarity of the CKM matrix. This leads to [7]

$$\sin 2\beta = 0.695 \pm 0.055 \quad (\text{from unitarity}). \quad (2)$$

which is in an excellent agreement with the value in Eq. (1) obtained from the CP asymmetries, and shows that the Standard Model can give a very consistent picture of CP violation and flavour changing weak interaction processes.

Results from the $B^0 \rightarrow \pi^+\pi^-$ decays are less consistent. BABAR [8] and BELLE [9] fit the two CP violation parameters $\mathcal{A}_{\pi^+\pi^-}^{\text{dir}}$ and $\mathcal{A}_{\pi^+\pi^-}^{\text{mix}}$ to the measured time-dependent CP asymmetries between \bar{B}^0 and B^0 decaying into $\pi^+\pi^-$ with the function

$$\mathcal{A}_{\pi^+\pi^-}^{\text{CP}}(t) = \mathcal{A}_{\pi^+\pi^-}^{\text{dir}} \cos(\Delta m_d t) + \mathcal{A}_{\pi^+\pi^-}^{\text{mix}} \sin(\Delta m_d t),$$

where Δm_d is the oscillation frequency. The results are

$$\mathcal{A}_{\pi^+\pi^-}^{\text{dir}} = \begin{cases} 0.30 \pm 0.25 & \text{BABAR} \\ 0.77 \pm 0.28 & \text{BELLE} \end{cases}$$

and

$$\mathcal{A}_{\pi^+\pi^-}^{\text{mix}} = \begin{cases} +0.02 \pm 0.34 & \text{BABAR} \\ -1.23 \pm 0.42 & \text{BELLE} \end{cases},$$

which do not allow us to draw a clear conclusion.

Unlike for the case of the $J/\psi K_S^0$ decays, a theoretical interpretation of $\mathcal{A}_{\pi^+\pi^-}^{\text{dir}}$ and $\mathcal{A}_{\pi^+\pi^-}^{\text{mix}}$ is not simple. In addition to the $\bar{b} \rightarrow \bar{u} + W^+$ tree process, the $\bar{b} \rightarrow \bar{d} + g(\gamma, Z^0)$ penguin process is expected to make a sizable contribution to the decay. Since the two processes have different phases, γ (the V_{ub} phase) and $-\beta$ respectively, we cannot extract γ and β without knowing the exact relative contributions of the two processes.

For many other B^\pm , B^0 and \bar{B}^0 decay modes, no further evidence of CP violation has been seen so far with the current statistics of the BABAR and BELLE experiments.

If indeed new physics such as SUSY is just around the corner, it must contribute to B^0 - \bar{B}^0 oscillations and various decay modes which are generated by the loop diagrams, e.g. penguins and boxes. Since CP violation is sensitive to the phases of couplings, it gives a unique opportunity to probe not only the strengths but also the phases of the new couplings.

If new particles contribute to B^0 - \bar{B}^0 oscillations, $|V_{td}|$ cannot be determined from the oscillation frequency. Similarly,

$$\phi_d = 2\beta$$

is no longer valid and β cannot be determined from the CP asymmetry in $J/\psi K_S^0$ decays. Therefore, neither Eq. (2) nor Eq. (1) will give the phase of V_{td} .

For a comprehensive study of CP violation including possible contributions from new physics, the B_s^0 meson plays an essential role. This can be demonstrated in the following example. The phase of V_{ub} can be measured in several ways:

1. A theoretically clean way to extract γ is to mix the two tree diagrams, $\bar{b} \rightarrow \bar{u} + W^+$ and $\bar{b} \rightarrow \bar{c} + W^+$. This can be done by studying the time-dependent rates of B_s^0 decaying into $D_s^+K^-$ and $D_s^-K^+$ and their CP-conjugated processes [10]. From them, one can extract $\phi_s + \gamma$ without any theoretical ambiguity. Here, ϕ_s is the phase of $B_s^0 - \bar{B}_s^0$ oscillations, which can be obtained from the time-dependent CP asymmetry of B_s^0 and \bar{B}_s^0 decaying into $J/\psi\phi$ (or other CP eigenstates produced by the $b \rightarrow c + W^-$ and $\bar{b} \rightarrow \bar{c} + W^+$ tree processes). Combining the two results, γ can be determined.
2. As already discussed, both $\bar{b} \rightarrow \bar{u} + W^+$ tree and $\bar{b} \rightarrow \bar{d} + g(\gamma, Z^0)$ penguin processes contribute to the decay of B^0 into $\pi^+\pi^-$. By replacing all the d and \bar{d} quarks by s and \bar{s} quarks, respectively, the tree and penguin processes generate K^+K^- decays for the B_s^0 meson. If we assume that the strong interaction dynamics remains invariant under this interchange (U-spin symmetry) [11], the relative contributions of the penguin process with respect to the tree process are identical for the $B^0 \rightarrow \pi^+\pi^-$ and $B_s^0 \rightarrow K^+K^-$ decays. Under this assumption, γ can be determined from the time-dependent CP asymmetry for B^0 and \bar{B}^0 decaying into $\pi^+\pi^-$ and that for B_s^0 and \bar{B}_s^0 decaying into K^+K^- . Using the ϕ_d and ϕ_s values obtained from the CP asymmetries measured with $B^0, \bar{B}^0 \rightarrow J/\psi K_S^0$ and $B_s^0, \bar{B}_s^0 \rightarrow J/\psi\phi$, respectively, the assumed U-spin symmetry can be tested as well.
3. Another opportunity for observing the interference between the two tree processes, $\bar{b} \rightarrow \bar{u} + W^+$ and $\bar{b} \rightarrow \bar{c} + W^-$, and thus extracting γ , is given by $D^0 - \bar{D}^0$ oscillations [12]. This can be done by measuring the time-integrated decay rates for $B^0 \rightarrow D^0 K^{*0}$, $B^0 \rightarrow \bar{D}^0 K^{*0}$, $B^0 \rightarrow D_{CP} K^{*0}$ and for their CP-conjugated processes, where D_{CP} denotes the CP eigenstate of the neutral D meson.

It is important to note that the γ measured in the first method will not be affected by the possible existence of new particles. The second method makes an explicit use of the penguin processes where new particles can contribute to the penguin loops. Therefore, the extracted value of γ could be affected by new physics. Equally for the third method, new physics in $D^0 - \bar{D}^0$ oscillations could affect the extracted value of γ . From these three γ measurements, we can

- determine γ and, together with the $|V_{ub}|$ measurements, extract the CKM parameters even in the presence of new physics, and
- extract the contribution of new physics to the oscillations and penguins.

Note that the Standard Model analysis using the present knowledge of $|V_{ub}|$, $|V_{cb}|$, $|V_{td}|$ and $\sin 2\beta$ predicts $\gamma \sim 65^\circ$ [7].

There are many other CP-violating decay modes where the extracted phases of V_{td} , V_{ub} and V_{ts} are affected differently by new physics. Studies of those decay modes with high accuracy will give us a different insight to the properties of the new physics, compared to what could be obtained from the direct search at ATLAS and CMS. As demonstrated, B_s^0 mesons play a crucial role here. This

gives a distinct advantage to hadron machines over e^+e^- B factories operating at the $\Upsilon(4S)$. Similarly, B_c^+ mesons and b baryons are also an exclusive domain of hadron machines. For interesting CP-violating B^0 decay modes such as $\pi^+\pi^-$, $K^\pm\pi^\mp$ and $K^{*0}\ell^+\ell^-$, the LHCb experiment will be able to collect several times more statistics in one year than that obtained by BABAR and BELLE by the time LHCb becomes operational.

2 Reoptimization of the detector

In order to achieve this physics goal, the LHCb detector must have a high track reconstruction efficiency, π -K separation capability from a few to ~ 100 GeV/c, very good proper-time resolution of ~ 40 fs and high trigger efficiencies, not only for final states including leptons but also for those with hadrons alone. The detector described in the Technical Proposal (TP) [13], approved in September 1998, was designed to fulfil those requirements.

At the time of the TP the material budget up to the second Ring Imaging Cherenkov detector (RICH 2) was 40% of X_0 (10% of λ_I), where X_0 (λ_I) is the radiation (nuclear interaction) length. This increased to 60% (20%) by the time the Outer Tracker Technical Design Report (TDR) [14] was submitted in September 2001, due to various technological constraints. Additional material deteriorates the detection capability of electrons and photons, increases the multiple scattering of charged particles, and increases occupancies of the tracking stations. With a larger fraction of nuclear interaction length, more kaons and pions interact before traversing the complete tracking system. The number of reconstructed B mesons therefore decreases, even if the efficiency of the tracking algorithm is maintained high for those tracks that do traverse the full spectrometer. This leads to a noticeable loss in the number of reconstructed B mesons from many-body final states. For example, one of the most promising CP violation measurements, from $B_s \rightarrow D_s K$ decays, requires five charged tracks (including one for tagging) to be reconstructed. For these reasons, an effort has been made to reduce the material budget back to the level at the time of the TP.

The trigger is one of the biggest challenges of the LHCb experiment [15]. It is designed to distinguish the events containing B mesons from the minimum-bias events through the presence of particles with a large transverse momentum (p_T) and the existence of secondary vertices. Events are first triggered by requiring at least one lepton or hadron with a p_T exceeding 1 to 3 GeV/c (Level-0) reducing the event rate to 1 MHz. It was realised that the robustness and efficiency of the second trigger level (Level-1) could be significantly improved by not only using information from the Vertex Locator (VELO), as done in the TP, but also adding p_T information to tracks with a large impact parameter. This can be achieved by associating the high- p_T calorimeter clusters and muons obtained at Level-0 to the tracks found in the VELO [15]. A complementary approach that is more efficient for hadrons is to get a rough p_T estimate from the tracking. This requires the introduction of a small amount of magnetic field in the region of RICH 1. The design of RICH 1 then has to be modified in order to protect its photon detectors from the field.

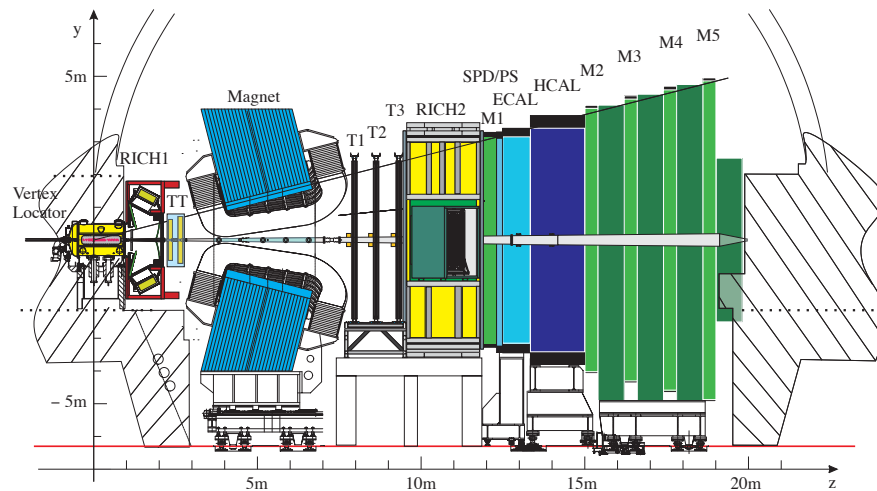


Fig. 1. Reoptimized LHCb detector layout, showing the Vertex Locator (VELO), the dipole magnet, the two RICH detectors, the four tracking stations TT and T1–T3, the Scintillating Pad Detector (SPD), Preshower (PS), Electromagnetic (ECAL) and Hadronic (HCAL) calorimeters, and the five muon stations M1–M5. It also shows the direction of the y and z coordinate axes; the x axis completes the right-handed framework.

3 Status of the LHCb detector

Figure 1 shows the layout of the reoptimized LHCb detector [16]. The basic layout of the spectrometer remains unchanged from that of the TP. It consists of the beam pipe, VELO, dipole magnet, tracking system, two Ring Imaging Cherenkov detectors with three radiators (RICH 1 and RICH 2), calorimeter system and muon system.

The exit window of the VELO vacuum tank will be made of 2mm Al and several prototypes are being fabricated for the vacuum test. The exit windows is connected to the first (25 mrad cone) section of the beam pipe. This will be made from pure beryllium and a prototype has been manufactured. The middle section (10 mrad cone) is foreseen to be made from beryllium-aluminium alloy, however it may also be changed to beryllium, depending on the price. The last section, passing through the calorimeter and muon systems, remains unchanged, made of stainless steel.

No major change in the VELO design has been introduced compared to the TDR [17]. The material budget has been reduced by optimizing the thickness of the silicon sensors and the number of stations. The thickness of the sensors has been reduced from 300 to 220 μm , and the number of stations from 25 to 21 without significantly affecting its performance.

The dipole magnet has not been modified from the TDR design [18]. The iron yoke plates and Al coils have been delivered and their assembly is advancing. Compared to the TP spectrometer layout, no shielding plate is placed upstream

of the magnet. This change has been made in order to introduce magnetic field between the VELO and the magnet, i.e. in the region of RICH 1, for the Level-1 trigger improvement.

Compared to the TP, the number of tracking stations is reduced to four in order to reduce the material budget, without introducing performance losses. The first station after the VELO, referred to as the Trigger Tracker (TT), is in front of the magnet and just behind RICH 1. It consists of four planes of silicon strip detectors. They are split into two pairs of planes separated by 30 cm. Together with the VELO, the TT is used in the Level-1 trigger. Large impact parameter tracks found in the VELO are extrapolated to the TT and the magnetic field in the RICH 1 region allows their momenta to be measured. The three remaining stations are placed behind the magnet with equal spacing. Each station consists of an Inner Tracker (IT) close to the beam pipe and an Outer Tracker (OT) surrounding the IT. The OT is made of straw tubes and the IT of silicon strip detectors. Their designs remain unchanged from those described in the corresponding TDR's [19, 14]. The engineering design of the Outer Tracker is completed and the construction is about to begin.

The RICH 1 material has been reduced, largely by changing the mirror material and redesigning the mirror support. The mirror will be made from either carbon-composite or beryllium. The mirror support has been moved outside of the acceptance. Further reduction of the material has been achieved by removing the entrance window, by connecting the front face of RICH 1 to the flange of the VELO exit window. Iron shielding boxes for the photon detectors have been introduced for two reasons. Firstly, they protect the photon detectors from the magnetic field. Secondly, they help to focus the magnetic field in the region where it is needed for the momentum measurement of the Level-1 trigger. In order to accommodate the shielding boxes, the optics has been changed introducing an additional flat mirror to the TDR design [20].

No design changes have been introduced for RICH 2 and the calorimeter system compared to the designs given in the TDR's [20, 21], and their construction is well advancing.

The muon system consists of five stations, M1 in front of the calorimeter system and M2–M5 behind the calorimeter, interleaved with iron shielding plates. In order to reduce the material budget seen by the calorimeter, M1 consists of two layers of Multi Wire Proportional Chambers, while the other four stations are made from four layers, as described in the TDR [22] and Addendum [23]. The construction of the chambers has started.

Figure 2 summarizes the material budget of the detector. The amount of material, as a fraction of radiation length, seen by a neutral particle from the nominal position of the primary vertex is plotted as a function of the pseudo-rapidity, η . The material is averaged over the azimuthal angle ϕ at three different z positions: 1) in front of the magnet, 2) in front of RICH 2 and 3) in front of the Calorimeter system. It shows that most of the particles see 20–30% of X_0 before entering the magnet. After the magnet, the three tracking stations lead to an additional $\sim 10\%$ of X_0 . Before reaching the calorimeter system, RICH 2 and the first muon station add another $\sim 30\%$. The fraction of interaction length in front of RICH 2 is now $\sim 12\%$ of λ_I .

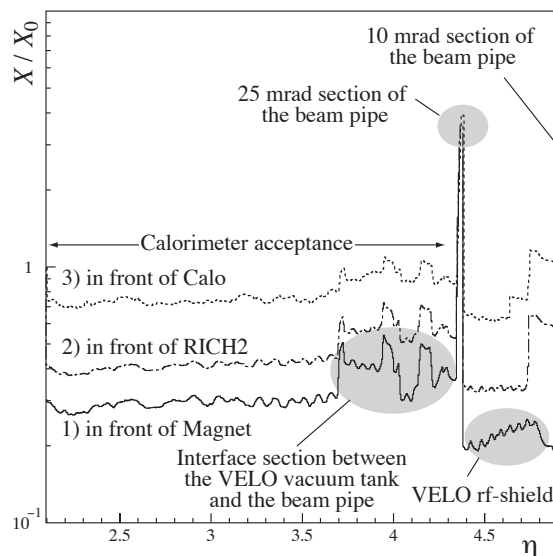


Fig. 2. Material seen by a neutral particle from the nominal position of the primary vertex as a function of the pseudo-rapidity at three different z positions, averaged over the azimuthal angle.

Note that details for the expected performance of the reoptimized detector on the trigger (A. Satta and T. Schietinger), particle identification (C. Jones), tracking (J. van Tilburg) and physics (M. Musy) are reported in these proceedings.

4 Conclusions

Reoptimization of the LHCb detector, which reduces the material budget and improves the trigger performance, has been successfully completed. The resulting detector fulfils the requirements given by the physics goals. The quark flavour changing process in the Standard Model can be tested in a unique way using many reconstructed B mesons from the different final states, beyond the capabilities of current experiments at the e^+e^- B factories and the Tevatron. The construction of the detector is advancing well and the full physics programme is expected to start when the LHC will become operational in 2007.

References

1. BABAR Collaboration, B. Aubert *et al.*, Phys. Rev. Lett. **87** (2001) 091801.
2. Belle Collaboration, K. Abe *et al.*, Phys. Rev. Lett. **87** (2001) 091802.
3. BABAR Collaboration, B. Aubert *et al.*, Phys. Rev. Lett. **89** (2002) 201802;
Belle Collaboration, K. Abe *et al.*, Phys. Rev. D **66** (2002) 071102.
4. L. Wolfenstein, Phys. Rev. Lett. **51** (1983) 1945.

5. M. Kobayashi and T. Maskawa, *Prog. Theor. Phys.* **49** (1973) 652.
6. N. Cabibbo, *Phys. Rev. Lett.* **10** (1963) 531.
7. For one of the most recent CKM analyses, see M. Battaglia *et al.*, “The CKM matrix and the unitarity triangle”, [arXiv:hep-ph/0304132](https://arxiv.org/abs/hep-ph/0304132), 2003.
8. BABAR Collaboration, B. Aubert *et al.*, *Phys. Rev. Lett.* **89** (2002) 281802.
9. Belle Collaboration, K. Abe *et al.*, *Phys. Rev. D* **68** (2003) 012001.
10. R. Aleksan, I. Dunietz and B. Kayser, *Z. Phys. C* **54** (1992) 653.
11. R. Fleischer, *Phys. Lett. B* **459** (1999) 306.
12. M. Gronau and D. Wyler, *Phys. Lett. B* **265** (1991) 172;
I. Dunietz, *Phys. Lett. B* **270** (1991) 75.
13. LHCb Collaboration, S. Amato *et al.*, Technical Proposal, CERN–LHCC/98–4.
14. LHCb Collaboration, P.R. Barbosa Marinho *et al.*, Outer Tracker Technical Design Report, CERN–LHCC/2001–24.
15. LHCb Collaboration, R. Antunes Nobrega *et al.*, Trigger Technical Design Report, CERN–LHCC/2003–31.
16. LHCb Collaboration, R. Antunes Nobrega *et al.*, Reoptimized LHCb Detector Technical Design Report, CERN–LHCC/2003–30.
17. LHCb Collaboration, P.R. Barbosa Marinho *et al.*, Vertex Locator Technical Design Report, CERN–LHCC/2001–11.
18. LHCb Collaboration, S. Amato *et al.*, Magnet Technical Design Report, CERN–LHCC/2000–7.
19. LHCb Collaboration, A. Franca Barbosa *et al.*, Inner Tracker Technical Design Report, CERN–LHCC/2002–29.
20. LHCb Collaboration, S. Amato *et al.*, RICH Technical Design Report, CERN–LHCC/2000–37.
21. LHCb Collaboration, S. Amato *et al.*, Calorimeter System Technical Design Report, CERN–LHCC/2000–36.
22. LHCb Collaboration, P.R. Barbosa Marinho *et al.*, Muon System Technical Design Report, CERN–LHCC/2001–10.
23. LHCb Collaboration, Addendum to the Muon System Technical Design Report, CERN–LHCC/2003–2.